tivation of PI 3-kinase could then serve to eliminate a Vav inhibitor and simultaneously produce activators of Vav GEF activity. Vav is a member of a large family of molecules containing a Dbl homology domain and a PH domain that could be similarly regulated (*1*). Ras activation of Rac is mediated by PI 3-kinase (*19*). Ras^{V12C40}, a Ras effector mutant that retains the ability to bind to and activate PI 3-kinase but not other Ras effectors (*19*, *20*, *21*), cooperated with wild-type Vav to induce membrane ruffling in REF-52 fibroblasts (Fig. 3), supporting our suggestion that Ras activation of Rac is mediated by a Dbl-related molecule. Furthermore, regulation through the Dbl homology and PH domains of Sos, a bifunctional GEF for both Ras and Rac, is apparently similar to the regulation that we have proposed for Vav (*22*). The regulation of Vav by both PI 3-kinase and a protein kinase is similar to the dual regulation of the PH domain containing protein kinase B (PKB/AKT) (*23*). Perhaps such dual regulation is a general feature of signaling molecules with PH domains.

REFERENCES AND NOTES

1. I. P. Whitehead, S. Campbell, K. L. Rossman, C. J. Der, *Biochim. Biophys. Acta* **1332**, F1 (1997).
2. M. J. Hart, A. Eva, T. Evans, S. A. Aaronson, R. A. Cerione, *Nature* **354**, 311 (1991).
3. J. Han *et al.*, *Mol. Cell. Biol.* **17**, 1346 (1997).
4. P. Crespo *et al.*, *Nature* **385**, 169 (1997).
5. R. Khosravi-Far *et al.*, *Mol. Cell. Biol.* **14**, 6848 (1994).
6. X. R. Bustelo *et al.*, *Oncogene* **9**, 2405 (1994).
7. T. L. Collins, M. Deckert, A. Altman, *Immunol. Today* **18**, 221 (1997).
8. C. J. Marshall, *Curr. Opin. Cell Biol.* **8**, 197 (1996).
9. J. E. Harlan, P. J. Hajduk, H. S. Yoon, S. W. Fesik, *Nature* **371**, 168 (1994).
10. M. Hyvonen *et al.*, *EMBO J.* **14**, 4676 (1995).
11. K. M. Ferguson, M. A. Lemmon, J. Schlessinger, P. B. Sigler, *Cell* **83**, 1037 (1995).
12. K. K. Reddy, M. Saady, G. Whited, J. R. Falck, *J. Org. Chem.* **60**, 3385 (1995).
13. M. P. Derman *et al.*, *J. Biol. Chem.* **272**, 6465 (1997).
14. J. Han and D. Broek, unpublished data.
15. L. E. Rameh *et al.*, *J. Biol. Chem.* **272**, 21999 (1997).
16. A. Toker and L. C. Cantley, *Nature* **387**, 673 (1997).
17. J. Han, unpublished data.
18. M. S. Deckert, S. Tartare-Deckert, C. Couture, T. Mustelin, A. Altman, *Immunity* **5**, 591 (1996).
19. P. Rodriguez-Viciana *et al.*, *Cell* **89**, 457 (1997).
20. M. A. White *et al.*, *ibid* **80**, 533 (1995).
21. T. Joneson, M. A. White, M. H. Wigler, D. Bar-Sagi, *Science* **271**, 810 (1996).
22. A. S. Nimnual, B. A. Yatsula, D. Bar-Sagi, *ibid.* **279**, XXX (1998).
23. D.Stokoe *et al.*, *ibid.* **277**, 567 (1997).
24. M. Raab, M. Yamamoto, C. E. Rudd, *Mol. Cell. Biol.* **14**, 2862 (1994).
25. Either C8PtdIns(4,5)P_2-NH_2 or C8PtdIns(3,4,5)P_3-NH_2 (250 μg) in 10 μl of 0.1 M sodium borate buffer (pH 8.5) was added to the dried ^{125}I-labeled Bolton-Hunter reagent (NEN, Boston, MA) and incubated for 15 min at 0°C. To obviate subsequent conjugation, we reacted any unreacted ester with 0.5 ml of 0.2 M of glycine in 0.1 M borate buffer (pH 8.5) for 5 min at 0°C. Gel filtration (Sephadex G-10; Pharmacia) was used to separate labeled phospholipids from the glycine conjugates and hydrolysis products. Thin-layer chromatography was used to identify fractions containing the iodinated phosphoinositides. His-tagged Vav protein (10 pmol) bound to Ni-agarose was incubated with 0, 1, 2.5, 5, 25, or 50 μM iodinated C8PtdIns(4,5)P_2 in 100 μl of 20 mM tris-HCl (pH 7.5), 50 mM NaCl, 5 mM $MgCl_2$, and 0.2% Triton X-100 for 2 hours at room temperature and washed twice with the same buffer. Bound iodinated C8PtdIns(4,5)P_2 was measured with a gamma counter. For the competitive binding assay, ^{125}I-C8PtdIns(3,4,5)P_3 was incubated with His-tagged Vav protein bound to Ni-agarose in the presence or absence of 50 μM C8PtdIns(4,5)P_2 or 50 μM C8PtdIns(3,4,5)P_3 in the same buffer mentioned above, and the amount of bound iodinated C8PtdIns(3,4,5)P_3 was measured. His-tagged Vav mutant proteins bound to Ni-agarose were used for incubation with ^{125}I-C8PtdIns(3,4,5)P_3, and bound C8PtdIns(3,4,5)P_3 was counted.
26. Vav expression constructs with point mutations in the PH domain were created by site-directed mutagenesis with polymerase chain reaction (PCR). Overlapping fragments of the Vav PH coding sequence were amplified by PCR from pMB24 (*3*), a plasmid encoding full-length mouse Vav, with primers containing the point mutations. The fragments were joined by a second round of PCR. The resulting PCR product was digested with Fse I and Nde I and subcloned into pMB24. We created the pRSET-Vav PH domain mutants by replacing the Bgl II fragment of pRSET-Vav(L) (*3*) with Bgl II fragments from pMB24 PH domain mutants. DNA sequence analysis of the final plasmids confirmed that the mutations indicated in the text were present.
27. His-tagged Vav protein (20 pmol) bound to Ni-agarose was washed with 10 mM Hepes (pH 7.0), 10 μM [γ-^{32}P]ATP, and 12 mM $MgCl_2$ and incubated with 5 ng of recombinant Lck tyrosine kinase (Upstate Biotechnology, Lake Placid, NY) for various incubation times at 37°C in the presence or absence of 50 μM C8PtdIns(4,5)P_2 or 50 μM C8PtdIns(3,4,5)P_3. Phosphorylated Vav proteins bound to Ni-agarose were then washed with 10 mM Hepes (pH 7.0) and 12 mM $MgCl_2$, and the resulting products were separated by SDS-PAGE. At completion of the kinase reactions, the stoichiometry of phosphate to Vav was determined to be about 0.4 to 1. For Lck phosphorylation of Vav protein used in GEF assays, a similar protocol was used except that Lck kinase purified from a baculovirus expression system (*24*) was used and the phosphorylated Vav protein was washed and resuspended in 50 mM tris-HCl (pH 7.5), 5 mM $MgCl_2$, 20 mM KCl, and 1 mM dithiothreitol.
28. Nuclear injection of REF-52 cells was performed as described (*21*). Ras^{V12C40} was expressed from the vector pSRalpha (*20*). Myc-tagged Vav was expressed from the vector pCDNA-3 (Invitrogen) into which the entire wild-type Vav coding region was inserted. For immunofluorescence, injected cells were fixed with 3.7% formaldehyde in phosphate-buffered saline for at least 1 hour at room temperature. Cells were permeabilized with acetone for 3 min at −20°C. Cover slips were incubated for 1 hour at room temperature with a mixture of fluorescein-labeled phalloidin (Molecular Probes) and mouse antibody to Ras (Transduction Labs, Lexington, KY) or mouse monoclonal antibody to Myc (9E10, Santa Cruz Biotechnology, Santa Cruz, CA) followed by rhodamine-conjugated goat antibody to mouse immunoglobulin G (Cappel, Cochranville, PA). The cells were photographed with a Zeiss fluorescence microscope with a chilled Argus charge-coupled-device camera (Hamamatsu).

29. We thank G. Bokoch, T. Roberts, and C. Rudd for providing reagents. Supported by NIH grants CA50261 (D.B.), CA71443 (M.A.W), and GM31278 (J.R.F).

29 September 1997; accepted 11 December 1997

Coupling of Ras and Rac Guanosine Triphosphatases Through the Ras Exchanger Sos

Anjaruwee S. Nimnual, Bogdan A. Yatsula, Dafna Bar-Sagi*

The Son of Sevenless (Sos) proteins control receptor-mediated activation of Ras by catalyzing the exchange of guanosine diphosphate for guanosine triphosphate on Ras. The NH_2-terminal region of Sos contains a Dbl homology (DH) domain in tandem with a pleckstrin homology (PH) domain. In COS-1 cells, the DH domain of Sos stimulated guanine nucleotide exchange on Rac but not Cdc42 in vitro and in vivo. The tandem DH-PH domain of Sos (DH-PH-Sos) was defective in Rac activation but regained Rac stimulating activity when it was coexpressed with activated Ras. Ras-mediated activation of DH-PH-Sos did not require activation of mitogen-activated protein kinase but it was dependent on activation of phosphoinositide 3-kinase. These results reveal a potential mechanism for coupling of Ras and Rac signaling pathways.

Ras guanine nucleotide binding proteins regulate cell growth through the activation of signaling pathways that control gene expression and actin polymerization (*1*, *2*). The effects of Ras on the actin cytoskeleton are mediated by Rac, another small guanine nucleotide binding protein (*3*), and Rac proteins function downstream of Ras in the pathways leading to cellular proliferation and oncogenic transformation (*4*–*7*). However, the mechanisms linking Ras activation to Rac activation are unknown.

In mammalian cells, growth factor–induced activation of Ras is mediated by the guanine nucleotide exchange factor Sos (*8*, *9*). Sos catalyzes the exchange of guanosine diphosphate (GDP) for guanosine triphosphate (GTP) on Ras through a central domain of about 400 amino acids that is highly conserved among guanine nucleotide exchange factors (GEFs) for Ras. The NH_2-terminal domain of Sos is about 600 amino acids long and contains regions of homology

Department of Molecular Genetics and Microbiology, State University of New York at Stony Brook, Stony Brook, NY 11794, USA.

*To whom correspondence should be addressed: E-mail: barsagi@asterix.bio.sunysb.edu

to Dbl (DH) and pleckstrin (PH) domains. Because Dbl family proteins function as GEFs for specific members of the Rho family of guanosine triphosphatase (GTPases) (*10, 11*), we tested whether the DH domain of Sos (DH-Sos) can function as an activator of Rac.

Stimulation of Rac results in activation of the c-Jun NH_2-terminal kinase (JNK) (*12, 13*). To test whether DH-Sos can activate JNK, we transfected COS-1 cells with expression plasmids encoding T7 epitope-tagged DH-Sos (*14*) and a FLAG epitope-tagged version of JNK1. JNK activity was assayed in an immunocomplex kinase assay with c-Jun coupled to glutathione S-transferase (GST–c-Jun) as a substrate (*15*). Expression of constitutively activated Rac in which amino acid 12 was substituted to Val (RacV12) induced a 25-fold activation of JNK (Fig. 1A), and expression of DH-Sos led to a 15-fold stimulation of JNK activity. Activation of JNK induced by DH-Sos was inhibited (80%) by coexpression of dominant negative Rac in which residue 17 was changed to Asn (RacN17), indicating that the stimulation of JNK by DH-Sos depends on the activation of Rac. Expression of DH-Sos had no effect on the activity of another mitogen-activated protein kinase family member, ERK (*16*).

To determine whether DH-Sos might activate Rac by functioning as a GEF, we tested the ability of DH-Sos to stimulate the dissociation of guanine nucleotide from Rac. Human kidney 293 cells were transfected with an expression plasmid encoding T7 epitope-tagged DH-Sos or control vector. Lysates prepared from the transfected cells were incubated with a GST-Rac1 fusion protein bound to [α-^{32}P]GTP, and guanine nucleotide exchange activity was determined by measuring the amount of [α-^{32}P]GTP that remained bound to GST-Rac1 (*17*). In the presence of lysates from cells expressing DH-Sos, the rate of release of guanine nucleotide from Rac was about twice as fast as that in the presence of lysates from control cells (Fig. 1B), making it probable that DH-Sos functions as a GEF for Rac. Attempts to express and purify recombinant DH-Sos were not successful, thus preventing analysis of GEF activity with purified proteins.

To investigate the specificity of DH-Sos GEF activity, we examined the effects of DH-Sos expression on the activity of Cdc42. Activation of JNK by DH-Sos was not affected by coexpression of the dominant negative Cdc42, Cdc42N17 (Fig. 1C). Moreover, lysates from cells expressing DH-Sos displayed no GEF activity toward GST-Cdc42 (Fig. 1D). Similarly, DH-Sos failed to stimulate guanine nucleotide exchange on RhoA (*18*). Together, these data suggest that DH-Sos has a preferential activity toward Rac.

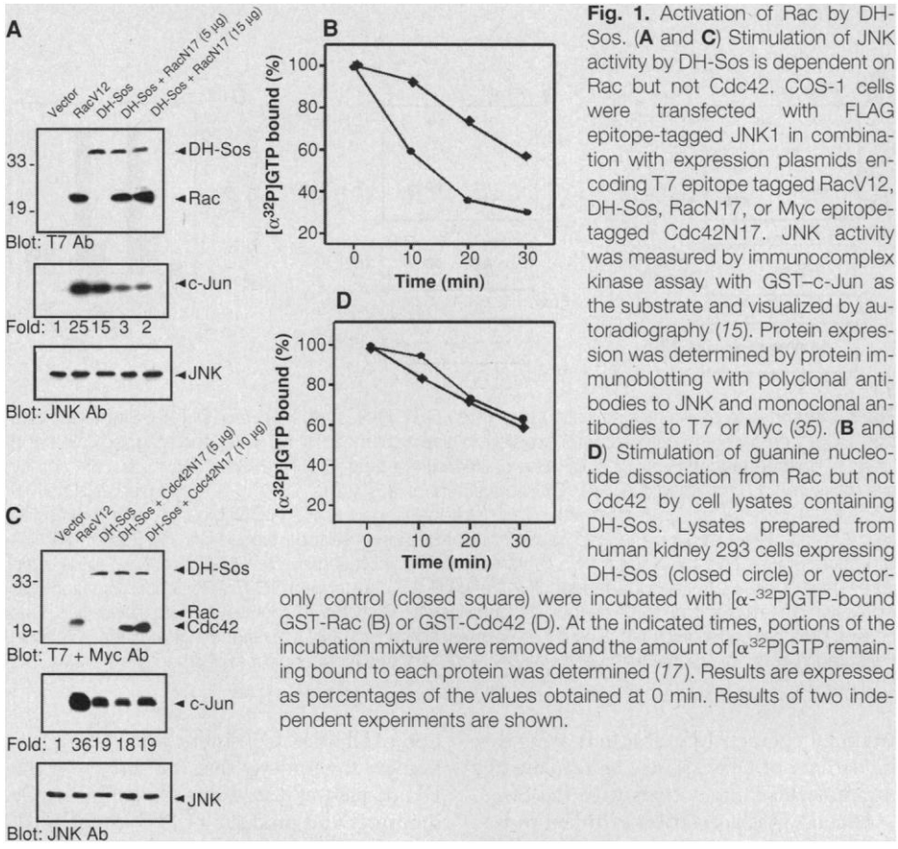

Fig. 1. Activation of Rac by DH-Sos. (**A** and **C**) Stimulation of JNK activity by DH-Sos is dependent on Rac but not Cdc42. COS-1 cells were transfected with FLAG epitope-tagged JNK1 in combination with expression plasmids encoding T7 epitope tagged RacV12, DH-Sos, RacN17, or Myc epitope-tagged Cdc42N17. JNK activity was measured by immunocomplex kinase assay with GST–c-Jun as the substrate and visualized by autoradiography (*15*). Protein expression was determined by protein immunoblotting with polyclonal antibodies to JNK and monoclonal antibodies to T7 or Myc (*35*). (**B** and **D**) Stimulation of guanine nucleotide dissociation from Rac but not Cdc42 by cell lysates containing DH-Sos. Lysates prepared from human kidney 293 cells expressing DH-Sos (closed circle) or vector-only control (closed square) were incubated with [α-^{32}P]GTP-bound GST-Rac (B) or GST-Cdc42 (D). At the indicated times, portions of the incubation mixture were removed and the amount of [α^{32}P]GTP remaining bound to each protein was determined (*17*). Results are expressed as percentages of the values obtained at 0 min. Results of two independent experiments are shown.

Rac proteins regulate the organization of the actin cytoskeleton, and activation of Rac induces polymerization of cortical actin and formation of membrane ruffles in fibroblasts (*3, 19*). We microinjected COS-1 cells with expression plasmids encoding T7 epitope-tagged wild-type Rac (RacWT) and DH-Sos (*20*). When microinjected alone, neither DH-Sos nor RacWT induced membrane ruffling (Fig. 2). However, membrane ruffling was observed when cells were injected with both RacWT and DH-Sos. DH-Sos differs from the DH domain of Tiam1, an activator of Rac, which requires an NH_2-terminal PH domain for induction of Rac-dependent membrane ruffling (*21*).

Most Dbl family members contain a DH domain in tandem with a PH domain (*10, 11*). In some cases, these PH domains have been shown to regulate the targeting of DH domains to the appropriate subcellular location (*21, 22*). The PH domain of Sos (PH-Sos) is located immediately to the COOH-terminal side of DH-Sos, binds phosphoinositides, and functions in membrane localization and activation of Sos (*23, 24*). To investigate the functional relationship between DH-Sos and PH-Sos, we analyzed the activity of a hemagglutinin (HA) epitope-tagged Sos construct containing the DH and PH domains (DH-PH-Sos) (*14*). When expressed in COS-1 cells, DH-PH-Sos failed to stimulate JNK activation (Fig. 3A). DH-PH-Sos did not induce membrane ruffling when microinjected either alone or with RacWT into quiescent COS-1 cells (*16*). Thus, the presence of the PH domain of Sos appears to inhibit the activity of the DH domain. The solution structure of the PH domain of Sos suggests that the PH and DH domains make specific

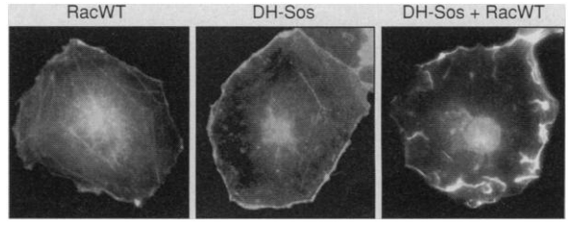

Fig. 2. Membrane ruffling induced by DH-Sos. Serum-deprived COS-1 cells were microinjected with expression plasmids encoding T7 epitope-tagged RacWT or DH-Sos or both, as indicated. Three hours after injection cells were fixed and stained with rhodamine-phalloidin to visualize membrane ruffles (*20*).

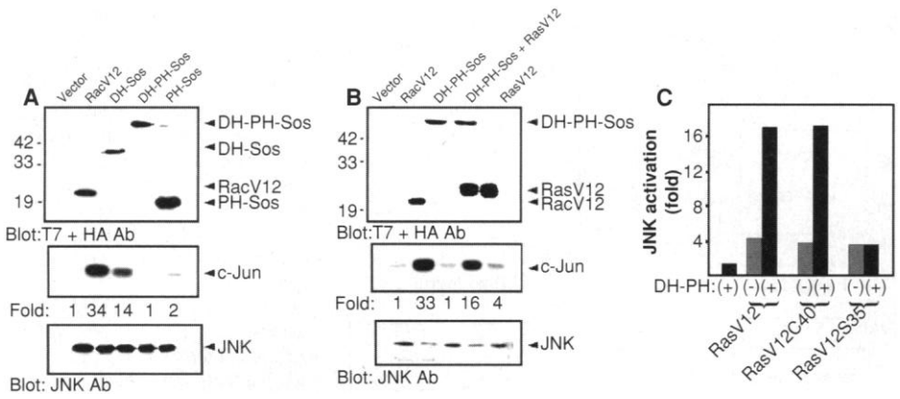

Fig. 3. Dependence on Ras for activation of JNK by DH-PH-Sos. (**A**) Failure of DH-PH-Sos to activate JNK. COS-1 cells were transfected with expression plasmids encoding FLAG epitope-tagged JNK1 and either T7 epitope-tagged RacV12 or DH-Sos or HA epitope-tagged DH-PH-Sos or PH-Sos. JNK activity was measured as described (Fig. 1A). (**B**) Requirement of RasV12 for DH-PH-Sos–induced JNK activation. COS-1 cells were transfected with FLAG epitope-tagged JNK1 in combination with expression plasmids encoding T7 epitope-tagged RacV12 or DH-Sos or HA epitope-tagged DH-PH-Sos or RasV12. (**C**) Effects of Ras effector binding loop mutants on JNK activation by DH-PH-Sos. COS-1 cells were cotransfected with FLAG epitope-tagged JNK1 and HA epitope-tagged DH-PH-Sos in combination with expression plasmids encoding HA epitope-tagged RasV12, RasV12C40, or RasV12S35. JNK activity was measured as described (Fig. 1A). Results are expressed as fold JNK activation relative to the activation measured in cells transfected with vector alone. Results of two independent experiments are shown.

structural contacts (*25*, *26*), indicating that the activity of DH-Sos may be regulated by intramolecular interactions with PH-Sos.

Because Ras activation is linked to Rac activation (*3*, *27*, *28*), we examined the role of Ras in DH-Sos–mediated activation of Rac. Coexpression of activated Ras, RasV12, with DH-Sos had no effect on the extent of JNK activation (*29*). However, DH-PH-Sos, which by itself failed to induce JNK activation (Fig. 3A), did activate JNK when it was coexpressed with RasV12 (Fig. 3B). Thus, Ras-dependent signals appear to enhance the activity of DH-Sos through a mechanism involving PH-Sos. We also tested the effects of Ras effector mutants that interact differentially with downstream effectors because of specific amino acid substitutions in the effector binding loop (*30*). The Ras mutant in which amino acid 35 was changed to Ser (RasV12S35) is able to bind to Raf-1 but not to RalGDS or the p110α subunit of phosphoinositide 3-kinase (PI 3-kinase), whereas the Ras mutant in which amino acid 40 was changed to Cys (RasV12C40) binds to p110α but not to Raf-1 and RalGDS (*28*, *31*). When expressed with DH-PH-Sos, only the RasV12C40 mutant enhanced activation of JNK (Fig. 3C). Thus, PI 3-kinase might be the effector by which Ras induces activation of DH-PH-Sos. The PH domain of Sos binds to the lipid product of PI 3-kinase phosphatidylinositol-3,4,5-trisphosphate [PtdIns(3,4,5)P_3] (*32*). Thus, activation of PI 3-kinase and the subsequent binding of PtdIns(3,4,5)P_3 to the PH domain could provide a mechanism for the activation of DH-Sos. Consistent with this suggestion are the findings that the activity of the DH domain of Vav is directly controlled by substrates and products of PI 3-kinase (*33*). A similar mode of regulation has been demonstrated for the PH domain of protein kinase B (*34*).

Our results suggest that Sos activates Ras through the Ras GEF domain and Rac through the DH domain. Ras-mediated PI 3-kinase signaling may provide a coupling mechanism by which Ras activation can control Rac activation. In support of such a mechanism is the observation that a Ras-induced actin rearrangement, which is mediated by Rac, requires functional PI 3-kinase acting upstream of Rac (*28*). Thus, the multidomain structure of Sos may allow the coordinated activation of signaling pathways involved in growth control and cytoskeletal organization.

REFERENCES AND NOTES

1. T. Joneson and D. Bar-Sagi, *J. Mol. Med.* **75**, 587 (1997).
2. C. J. Marshall, *Curr. Op. Cell Biol.* **8**, 197 (1996).
3. A. J. Ridley, H. F. Paterson, C. L. Johnston, D. Diekmann, A. Hall, *Cell* **70**, 401 (1992).
4. R.-G. Qiu, J. Chen, D. Kirn, F. McCormick, M. Symons, *Nature* **374**, 457 (1995).
5. R. Khosrovi-Far, P. Solkki, G. Clark, M. Kinch, C. Der, *Mol. Cell Biol.* **15**, 6443 (1995).
6. T. Joneson, M. A. White, M. H. Wigler, D. Bar-Sagi, *Science* **271**, 810 (1996).
7. J. Westwick *et al.*, *Mol. Cell. Biol.* **17**, 1324 (1997).
8. D. Bar-Sagi, *Trends Endocrinol.* **5**, 165 (1994).
9. R. Khosravi-Far and C. J. Der, *Cancer Metastasis Rev.* **13**, 67 (1994).
10. R. A. Cerione and Y. Zheng, *Curr. Op. Cell Biol.* **8**, 216 (1996).
11. I. P. Whitehead, S. Campbell, K. L. Rossman, C. Der, *Biochim. Biophys. Acta* **1332**, F1 (1997).
12. O. A. Coso *et al.*, *Cell* **81**, 1137 (1995).
13. A. Minden, A. Lin, F.-X. Claret, A. Abo, M. Karin, *ibid.*, p. 1147.
14. DH-Sos DNA was generated by polymerase chain reaction (PCR) amplification of hSos1 template with oligonucleotides 5′-CCGGTTAACGTAGAAGATATTAATATA-3′ and 5′-CCGGGATCCCTAATTACAACACTGTCCAATGTC-3′, which correspond to the sequences between nucleotide positions 538 to 555 and 1306 to 1326, respectively, of hSos1. The amplified fragment was ligated into T7 epitope-tagged pCMG6KR mammalian expression vector. DH-PH-Sos1 was generated by PCR amplification of a hSos1 template using oligonucleotides 5′-CCGTCTAGAGTAGAAGATATTAAT-3′ and 5′-CAAGGTACCTCATTCCAGTGTACTCCG-3′, which correspond to the sequences between nucleotide positions 538 to 552 and 1639 to 1653, respectively, of hSos1. The amplified fragment was ligated into HA epitope-tagged pCGN mammalian expression vector. Other expression vectors used in this study are described in (*6*).
15. COS-1 cells were transfected with expression plasmids by the calcium phosphate precipitation method. Transfected cells were collected in ice-cold lysis buffer [10 mM Hepes (pH 7.5),150 mM NaCl,10% (w/v) glycerol, 0.5% Triton X-100, 50 mM NaF, 50 μM Na_3VO_4, 0.2 mM phenylmethylsulfonyl fluoride (PMSF), 10 mM benzamidine, 0.02 mM leupeptin, trypsin inhibitor (10 μg/ml), aprotinin (10 μg/ml)] and portions of the cell lysates were removed for analyses of protein expression by immunoblotting. FLAG-tagged JNK1 was immunoprecipitated with M2 monoclonal antibody to FLAG (Kodak Scientific Imaging Systems). Immunocomplexes were collected by incubation with protein G-Sepharose, washed extensively with lysis buffer, and then incubated for 30 min at 30°C in kinase assay buffer [20 mM Hepes (pH 7.5), 20 mM $MgCl_2$, 20 mM β-glycerophosphate, 0.1 mM Na_3VO_4, 2 mM dithiothreitol (DTT), and 20 μM adenosine triphosphate (ATP)] containing GST c-Jun (3 μg) and 10 μCi of [γ-^{32}P]ATP (7000 Ci/mmol) (ICN). The reaction products were resolved on SDS-polyacrylamide gels, visualized by autoradiography, and quantified with a PhosphorImager.
16. A. Nimnual and D. Bar-Sagi, unpublished observation.
17. Human kidney 293 cells were transfected with DH-Sos or vector alone (control) and cells were harvested 24 hours after transfection. Cells were lysed by sonication in 300 μl of lysis buffer [20 mM tris-HCl (pH 8), 100 mM NaCl, 1 mM $MgCl_2$, 200 mM sucrose, 0.1 mM EDTA, 1 mM DTT, 0.5 mM PMSF, leupeptin (10 μg/ml), aprotinin (10 μg/ml)]. The homogenates were clarified by centrifugation at 100,000*g* for 20 min at 4°C. Purified GST-Rac and Cdc42 (50 pmol) were incubated with [α-^{32}P]GTP (100 pmol, 800 Ci/mmol) in 30 μl of buffer [25 mM tris-HCl (pH 7.5), 1 mM DTT, bovine serum albumin (10 mg/ml), 5 mM EDTA] for 30 min at 30°C. The bound [α-^{32}P]GTP was stabilized by the addition of $MgCl_2$ (final concentration, 10 mM). The exchange reaction was initiated by the addition of cell lysates (150 μl, 6 mg of proteins per milliliter) supplemented with 10 mM $MgCl_2$ and 2 mM guanosine 5′-*o*-(3′-thiotriphosphate). At the indicated times, portions (30 μl) were removed from the reaction mixture and diluted with 500 μl of ice-cold buffer [20 mM tris-HCl (pH 8), 100 mM NaCl, 20 mM $MgCl_2$]. The GST fusion proteins were isolated by precipitation with glutathione Sepharose and bound nucleotides were eluted with 1% SDS and 20 mM EDTA for 5 min at 65°C. Radioactivity was quantified by scintillation counting.
18. D. Broek, personal communication.
19. C. D. Nobes and A. Hall, *Cell* **81**, 53 (1995).
20. COS-1 cells were plated onto glass coverslips and cultured in Dulbecco's modified Eagle's medium (DMEM) containing fetal bovine serum (5%). Three hours before injection, cells were placed in serum-free DMEM. Plasmid mixtures containing the indicated plasmids in microinjection buffer [50 mM Hepes (pH 7.2), 100 mM KCl, 5 mM $NaHPO_4$] were microinjected into cell nuclei. Three hours after injection, cells were fixed with 3.7% formaldehyde in phos-

phate-buffered saline for 1 hour, then permeabilized with 0.1 % Triton X-100 for 3 min, and incubated for 1 hour with rhodamine-conjugated phalloidin (Molecular Probes). The cells were photographed with a Zeiss Axiovert microscope.
21. F. Michiels *et al.*, *J. Cell Biol.* **137**, 387 (1997).
22. Y. Zheng, D. Zangrilli, R. A. Cerione, E. Alessandra, *J. Biol. Chem.* **271**, 19017 (1996).
23. R.-H. Chen, S. Corbalan-Garcia, D. Bar-Sagi, *EMBO J.* **16**, 1351 (1997).
24. L. McCollam *et al.*, *J. Biol. Chem.* **270**, 15954 (1995).
25. J. Zheng *et al.*, *J. Cell Biol.* **272**, 30340 (1997).
26. S. Koshiba *et al.*, *J. Mol. Biol.* **269**, 579 (1997).
27. T. Joneson, M. McDonough, D. Bar-Sagi, L. Van Aelst, *Science* **274**, 1374 (1996).
28. P. Rodriguez-Viciana *et al.*, *Cell* **89**, 457 (1997).
29. B. Yatsula and D. Bar-Sagi, unpublished observation.
30. M. A. White *et al.*, *Cell* **80**, 533 (1995).
31. R. Khosravi-Far *et al.*, *Mol. Cell Biol.* **16**, 3923 (1996).
32. L. E. Rameh *et al.*, *J. Biol. Chem.* **272**, 21999 (1997).
33. J. Han *et al.*, *Science* **279**, 558 (1998).
34. D. Stokoe *et al.*, *ibid.* **277**, 567 (1997).
35. Proteins were fractionated by SDS–polyacrylamide gel electrophoresis and electrophoretically transferred to nitrocellulose membrane (Schleicher & Schuell) at a constant voltage of 90 V for 45 min in transfer buffer [25 mM tris-HCl, 192 mM glycine, 20% (v/v) methanol]. The membranes were incubated with monoclonal antibody to T7 (Novagen), monoclonal antibody to HA (12CA5) (Babco), monoclonal antibody to Myc (9E10), or polyclonal antibody to JNK1 (Santa Cruz Biotechnology) for 1 hour and then with horseradish peroxidase–conjugated goat antibody to mouse immunoglobulin G (IgG) or goat antibody to rabbit IgG (Cappel). The immunoreactive bands were visualized with the enhanced chemiluminescence detection system (Dupont-NEN).
36. We thank A. Hall and R. Cerione for plasmids. Supported by National Institutes of Health grants CA28146 and CA55360. A.S.N. and B.A.Y. are supported by National Institutes of Health training grant CA09176.

23 September 1997; accepted 11 December 1997

Plasma Insulin-Like Growth Factor–I and Prostate Cancer Risk: A Prospective Study

June M. Chan,* Meir J. Stampfer, Edward Giovannucci, Peter H. Gann, Jing Ma, Peter Wilkinson, Charles H. Hennekens, Michael Pollak

Insulin-like growth factor–I (IGF-I) is a mitogen for prostate epithelial cells. To investigate associations between plasma IGF levels and prostate cancer risk, a nested case-control study within the Physicians' Health Study was conducted on prospectively collected plasma from 152 cases and 152 controls. A strong positive association was observed between IGF-I levels and prostate cancer risk. Men in the highest quartile of IGF-I levels had a relative risk of 4.3 (95 percent confidence interval 1.8 to 10.6) compared with men in the lowest quartile. This association was independent of baseline prostate-specific antigen levels. Identification of plasma IGF-I as a predictor of prostate cancer risk may have implications for risk reduction and treatment.

The cell proliferation rate is positively correlated with the risk of transformation of certain epithelial cells (*1*). Insulin-like growth factors have mitogenic and antiapoptotic effects on normal and transformed prostate epithelial cells (*2–4*). Most circulating IGF-I originates in the liver, but IGF bioactivity in tissues is related not only to circulating IGF and IGF binding protein (IGFBP) levels, but also to local production of IGFs, IGFBPs, and IGFBP proteases (*5*). Person-to-person variability in levels of plasma IGF-I and IGFBP-3 [the major circulating IGFBP (*5*)] is considerable (*6, 7*), and plasma IGF-I levels appear to reflect heterogeneity in tissue IGF-I bioactivity (*8–11*).

To examine the potential relation between plasma IGF-I, IGF-II, and IGFBP-3 levels and prostate cancer risk, we conducted a prospective case-control study of men participating in the Physicians' Health Study (*12*). At the start of the study (1982), the men (aged 40 to 82) provided medical information via mailed-in questionnaires, and 14,916 (68%) also provided plasma (*12*). Through 1992 follow-up was over 99% complete. Reports of prostate cancer were verified by medical records (*13*).

Cases and controls were selected from the 14,916 physicians who provided plasma. By March 1992, we confirmed 520 cases, of whom 152 had adequate volume for IGF assays in 1997. Levels of plasma steroid hormones (*14*), prostate-specific antigen (PSA) (*15*), and carotenoids, and CAG polymorphisms of the androgen receptor gene (*16*) had previously been measured in the same samples (*17*). On average, 7 years (minimum = 6 months, maximum = 9.5 years) elapsed between plasma collection and diagnosis.

We selected controls at random from men who provided blood and had not reported a diagnosis of prostate cancer up to the diagnosis date of the case. We excluded men with inadequate sample volume and who had total or partial prostatectomies by the time of the case diagnosis. We matched one control to each case on the basis of smoking (never, past, or current), duration of follow-up, and age within 1 year.

IGF-I, IGF-II, and IGFBP-3 were assayed by enzyme-linked immunoabsorbent assay (ELISA) with reagents from Diagnostic Systems Laboratory (Webster, Texas) (*18, 19*). A single IGF-I measurement is generally representative of levels over time (*20, 21*). We used paired *t* tests to compare the means of IGF-I, IGF-II, and IGFBP-3 levels between cases and controls. We examined age-standardized (using five groups: 40 to 50, 51 to 55, 56 to 60, 61 to 65, and 66 to 80) mean values of various predictors for prostate cancer within quartiles of IGF-I among the controls. Conditional logistic regression was used to analyze the associations between IGF and prostate cancer, after adjustment for other possible risk factors—PSA, height, weight, body mass index, CAG polymorphisms of the androgen receptor gene, and plasma levels of lycopene, estrogen, testosterone (T), dihydrotestosterone (DHT), sex hormone binding globulin (SHBG), prolactin, and 3α-androstanediol glucuronide (AAG) (*14–16, 22–24*). In view of the growth-inhibitory properties of IGFBP-3 and its potential to reduce the bioactivity of IGF (*25*), we hypothesized that high levels of IGFBP-3 would be inversely related to risk. Because levels of IGF-I and IGFBP-3 were highly correlated, it was necessary to simultaneously adjust for these factors in regression models to observe their independent effects.

We estimated relative risks (RRs) from the odds ratios and computed 95% confidence intervals (CIs) (*24*). In stratified analyses, we used unconditional logistic regression models and adjusted for age (eight 5-year categories) and smoking (never, past, and current) in the models to make full use of the data without restriction to the matched pairs (*24*). We also separately examined high grade/stage cases, low grade/

J. M. Chan and M. J. Stampfer, Department of Epidemiology, Harvard School of Public Health, 677 Huntington Avenue, Boston, MA 02115, USA.
E. Giovannucci and J. Ma, Channing Laboratory, Department of Medicine, Brigham and Women's Hospital, Harvard Medical School, Boston, MA 02115, USA.
P. H. Gann, Department of Preventive Medicine, Northwestern University Medical School, Chicago, IL 60611, USA.
P. Wilkinson and M. Pollak, Cancer Prevention Research Unit, Departments of Medicine and Oncology, Lady Davis Research Institute of the Jewish General Hospital and McGill University, Montreal, Canada H3T1E2.
C. H. Hennekens, Division of Preventive Medicine, Department of Medicine and Department of Ambulatory Care and Prevention, Brigham and Women's Hospital and Harvard Medical School, Boston, MA 02115, USA.

*To whom correspondence should be addressed. E-mail: jmlchan@hsph.harvard.edu